INT. J. REMOTE SENSING, 2002, VOL. 23, NO. 15, 3009–3022

Observation of flooding and rice transplanting of paddy rice fields at the site to landscape scales in China using VEGETATION sensor data

X. XIAO*, S. BOLES, S. FROLKING, W. SALAS, B. MOORE III, C. LI

Complex Systems Research Center, Institute for the Study of Earth, Oceans and Space, University of New Hampshire, Durham, NH 03824, USA

L. HE and R. ZHAO

Nanjing Institute of Geography and Limnology, Chinese Academy of Sciences, Nanjing, China

(*Received 23 June 2000; in final form 22 May 2001*)

Abstract. A unique physical feature of paddy rice fields is that rice is grown on flooded soil. During the period of flooding and rice transplanting, there is a large proportion of surface water in a land surface consisting of water, vegetation and soils. The VEGETATION (VGT) sensor has four spectral bands that are equivalent to spectral bands of Landsat TM, and its mid-infrared spectral band is very sensitive to soil moisture and plant canopy water content. In this study we evaluated a VGT-derived normalized difference water index ($NDWI_{VGT} = (B3 - MIR)/(B3 + MIR)$) for describing temporal and spatial dynamics of surface moisture. Twenty-seven 10-day composites (VGT- S10) from 1 March to 30 November 1999 were acquired and analysed for a study area (175 km by 165 km) in eastern Jiangsu Province, China, where a winter wheat and paddy rice double cropping system dominates the landscape. We compared the temporal dynamics and spatial patterns of normalized difference vegetation index ($NDVI_{VGT}$) and $NDWI_{VGT}$. The $NDWI_{VGT}$ temporal dynamics were sensitive enough to capture the substantial increases of surface water due to flooding and rice transplanting at paddy rice fields. A land use thematic map for the timing and location of flooding and rice transplanting was generated for the study area. Our results indicate that NDWI and NDVI temporal anomalies may provide a simple and effective tool for detection of flooding and rice transplanting across the landscape.

1. Introduction

Paddy rice agriculture is one of the major cropping systems in Asia. It is estimated that in 1990 China had a total area of 33 Mha of paddy rice fields, and a total rice yield of 192 million metric tons, accounting for about 37% of the world's rice production (Zhao *et al.* 1996). Paddy rice fields provide essential food for billions of people in the world, but also are a significant source of greenhouse gases, particularly methane (Neue and Boonjawat 1998, Denier van der Gon 2000), which may have substantial impacts on atmospheric chemistry and climate.

*e-mail: xiangming.xiao@unh.edu

International Journal of Remote Sensing
ISSN 0143-1161 print/ISSN 1366-5901 online © 2002 Taylor & Francis Ltd
http://www.tandf.co.uk/journals
DOI: 10.1080/01431160110107734

A unique physical feature of paddy fields is that the rice is grown on flooded soils. Temporal development of paddy rice fields can be characterized by three main periods: (1) the flooding and rice transplanting period; (2) the growing period (vegetative growth stage, reproductive stage and ripening stage); and (3) the fallow period after harvest (Le Toan *et al.* 1997). Emissions of methane (CH_4) from paddy rice fields begin immediately after flooding. The timing of flooding and rice transplanting at paddy rice fields varies across landscape and regional scales, and indicates the beginning of the paddy rice growing cycle. Therefore, updated information on (1) the timing of flooding and rice transplanting of paddy rice fields, and (2) the area and distribution of paddy rice fields, is needed in order to better quantify the impact of paddy rice agriculture on atmospheric chemistry and climate. Updated information on the temporal characteristics of paddy rice fields also has the potential to improve predictions of leaf area index and biomass/yields using spectral vegetation indices and agro-ecosystem models (Gao *et al.* 1992, Miller *et al.* 1993, Wang *et al.* 1996).

A number of studies have used optical remote sensing data (Landsat TM, Advanced Very High Resolution Radiometer, {AVHRR}) to estimate the areas of paddy rice fields (Martin and Heilman 1986, Tennakoon *et al.* 1992, Bachelet 1995, Okamoto and Fukuhara 1996, Lu 1997, Fang 1998, Fang *et al.* 1998, Okamoto and Kawashima 1999). However, no studies have directly used optical sensor data to estimate the timing of flooding and transplanting of paddy rice fields at landscape to regional scales because of limitations of both Landsat TM and AVHRR data. Landsat TM imagery has fine spatial resolution (30 m), but its long revisit cycle (16-days) and frequent cloud cover in paddy rice growing areas make it difficult to acquire multi-temporal cloud-free images for identifying the flooding and rice transplanting at paddy rice fields. The AVHRR instrument has a daily revisit cycle, but its lack of a mid-infrared spectral band that is sensitive to changes in soil moisture and vegetation canopy moisture makes it incapable of directly identifying the flooding and rice transplanting at paddy rice fields (table 1).

The SPOT-4 satellite, which was launched in March 1998, carries the VEGETATION (VGT) instrument and the high-resolution visible and infrared (HRVIR) instrument. The VGT instrument has four spectral bands that are equivalent to spectral bands of Landsat TM (table 1). The VGT blue band is mostly used for atmospheric corrections, and the mid-infrared band (MIR) is highly sensitive to soil moisture content, vegetation cover and leaf moisture content. The sensitivity of the MIR band to the water content of the land surface makes it easier to accurately locate surface water, as water completely absorbs mid-infrared radiation. The VGT instrument also provides daily images of the global land surface at 1-km spatial

Table 1. A comparison of VEGETATION (VGT) in SPOT-4, Landsat TM and AVHRR sensors.

VGT (nm)	TM (nm)	AVHRR-11 (nm)
B0 (430–470) blue	TM1 (450–520)	
B2 (610–680) red	TM3 (630–690)	CH1 (580–680)
B3 (780–890) near-infrared	TM4 (760–900)	CH2 (725–1100)
MIR (1580–1750) mid-infrared	TM5 (1550–1750)	
Spatial resolution: 1 km	Spatial resolution: 30 m	Spatial resolution: 1-km
Revisit time: daily	Revisit time: 16-days	Revisit time: daily

resolution. Therefore, VGT data have the potential for detection of flooding and transplanting of paddy rice fields across landscape and regional scales.

In this study we analysed multi-temporal 10-day VGT synthesis products acquired from 1 March to 30 November 1999. The study area is located in eastern Jiangsu Province, China (figure 1), where agriculture is dominated by winter wheat/paddy rice and rapeseed/paddy rice double cropping rotation systems. Immediately after the harvest of winter wheat and rapeseed crops in late May and early June, farmers begin land preparation/flooding/rice transplanting of paddy rice fields. Our objective was to assess the potential of multi-temporal VGT data for identifying the timing and extent of flooding and rice transplanting at the scales of farm and landscape.

2. Remote sensing data and vegetation indices

SPOT Image Inc. provides three standard VGT products to users: VGT-P (physical product), VGT-S1 (daily synthesis product) and VGT-S10 (10-day synthesis

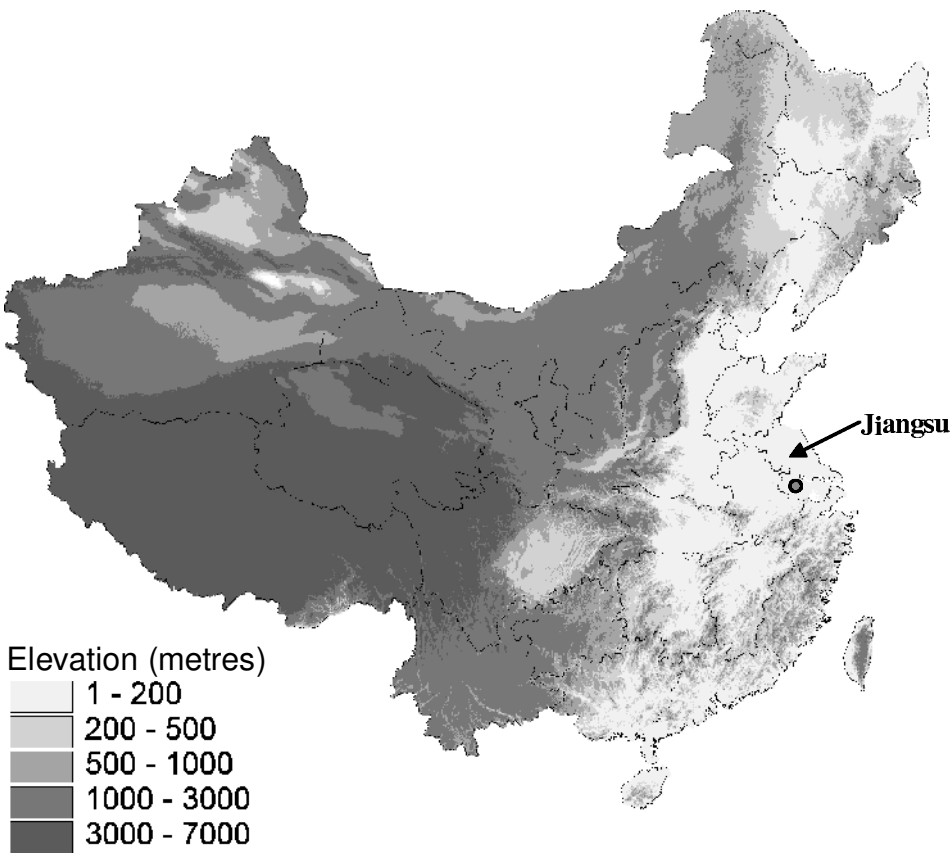

Figure 1. The location of the study area (filled circle) in Jiangsu Province, China. The background is the digital elevation model (DEM) at 1-km spatial resolution (from the USGS Global 30 Arc Second Elevation Data Set, http://edcwww.cr.usgs.gov/landdaac/gtopo30/gtopo30.html). The polygons are the province boundary map of China (in 1990) at 1:1 000 000 scale. Both the DEM and province boundary map are in Lambert Azimuthal Equal Area projection.

product). For each month there are three 10-day composites: days 1–10, days 11–20 and day 21 to the last day of a month. VGT-S10 data are generated using the composite approach, which is based on the maximum Normalized Difference Vegetation Index (NDVI) values within a 10-day period for a pixel, which helps minimize the effect of cloud cover and variability in atmospheric optical depth. The four spectral bands (B0, B2, B3, MIR, see table 1) in the VGT-S10 products are the estimates of ground surface reflectance, as atmospheric corrections for ozone, aerosols and water vapour have already been applied to the VGT images using the SMAC algorithm (Rahman and Dedieu 1994). The ground surface reflectance values of the four spectral bands were used in data analysis. Twenty-seven VGT-S10 products from 1–10 March to 21–30 November 1999 for the study area were used in this study.

Tucker (1980) suggested that the mid-infrared band (TM5) of Landsat TM was best suited for space-borne remote sensing of plant canopy water content. Gao (1996) proposed the Normalized Difference Water Index (NDWI) for remote sensing of vegetation liquid water from space, using reflectance values of two near-infrared bands (one band centred at approximately 860 nm, the other at 1240 nm). NDWI was considered to be a complementary vegetation index to the NDVI (Gao 1996). In this study, NDWI and NDVI were calculated for each of the VGT-S10 products, using the ground surface reflectance values of the spectral bands:

$$\mathrm{NDWI}_{\mathrm{VGT}} = (\mathrm{B3} - \mathrm{MIR})/(\mathrm{B3} + \mathrm{MIR}) \quad (1)$$

$$\mathrm{NDVI}_{\mathrm{VGT}} = (\mathrm{B3} - \mathrm{B2})/(\mathrm{B3} + \mathrm{B2}) \quad (2)$$

3. The study area in eastern Jiangsu Province, China

For the landscape-scale analysis in this study, we used a subset (175 pixels × 165 pixels) of VGT-S10 data that coincides spatially with a Landsat TM image (Path 120 and Row 38) acquired on 22 April 1996. The study area is located in eastern Jiangsu Province, including Nanjing City and Jiangning County (figures 1 and 2(a)). Elevation in the study area varies from 1 to 500 m. Out of a total area of 28 875 km^2, approximately 95.3% of the land is at an elevation of less than 100 m and 86.5% of the land is at an elevation of less than 50 m (figure 2(*b*)). The Yangtze River flows through the study area and other surface water bodies include lakes and numerous fish and aquaculture ponds (figure 2(*c*)). Agriculture in the study area is dominated by double cropping systems that consist of either winter wheat and paddy rice or rapeseed and paddy rice. Croplands (figure 2(*d*)) are mostly distributed in low elevation and flat plain areas. The pink to red colours in the VGT composite graph (figure 2(*a*)) correspond well with the spatial distribution of croplands (figure 2(*d*)) derived from Landsat TM imagery at 30-m spatial resolution.

In 1999 five intensive sampling sites were set up in Jiangning County (figure 3). Jiangning County is south of Nanjing City, and is in the middle of the landscape-scale study area (figure 2(*a*)). In Jiangning County, every farm family has about 3–5 mu (1 ha = 15 mu) of paddy rice field, depending on family size. Each of the five sampling sites belongs to one farm family. Each field site was selected to lie within a 2–3 km^2 landscape dominated by paddy rice fields (over 90% of the area). We used a hand-held global positioning system (GPS) receiver to locate the latitude and longitude positions of the five sampling sites. The field-collected geographical information was used to locate each of the sampling sites in the VGT images and we then extracted both the NDVI and NDWI time series data for these five sampling sites. According to the VEGETATION User Guide, the geometric accuracy of VGT

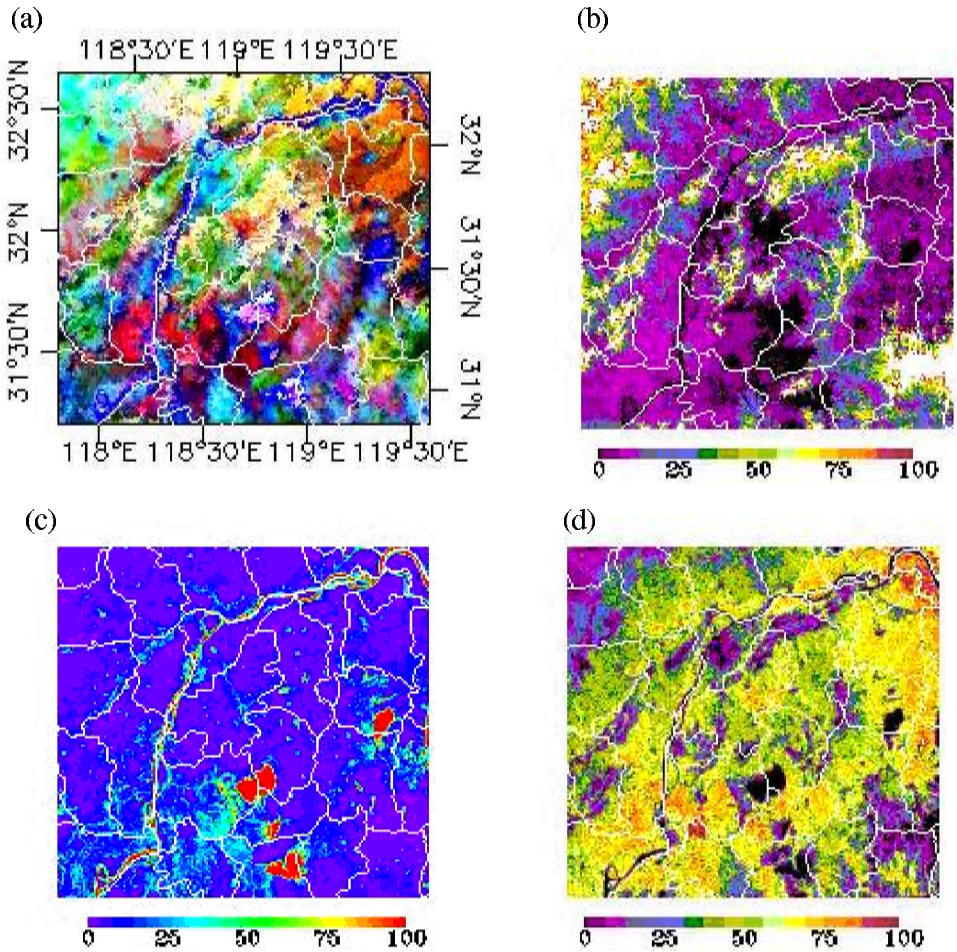

Figure 2. Land cover characteristics of the study area in eastern Jiangsu Province, China. (*a*) False colour composite of VEGETATION 10-day composite data on 21–30 April 1999, using spectral bands B3 (red), MIR (green) and B2 (blue). (*b*) Elevation at 1-km resolution. (*c*) Percentage water body within a 1-km^2 pixel, as aggregated from Landsat TM image (30-m resolution) classification. (*d*) Percentage cropland area within a 1-km^2 pixel, as aggregated from Landsat TM image (30-m resolution) classification. The TM image was acquired on 26 April 1996 and the detailed TM image classification is reported in another paper (Xiao *et al.* 2002b). The TM image, DEM and VGT data were co-registered and are in Lambert Azimuthal Equal Area projection. The polygons are the county boundary map at 1:1 000 000 scale.

data has an absolute location error of < 0.8 km, therefore, we expect that the selected VGT image pixels contain the field sampling sites.

For the five sampling sites, the cropping system in 1999 was a winter wheat and paddy rice rotation. Winter wheat crops had been planted after the harvest of paddy rice crops in October 1998. After a brief growing period, winter wheat crops over-wintered, and then commenced vigorous growth in the spring of 1999. By late May, wheat crops ripened and were ready for harvest (figure 4(*a*)). Following the harvest of winter wheat, stubble was typically burned and then, within 1–2 weeks, fields were ploughed and flooded (figure 4(*b*)). Flooding is one key practice of paddy

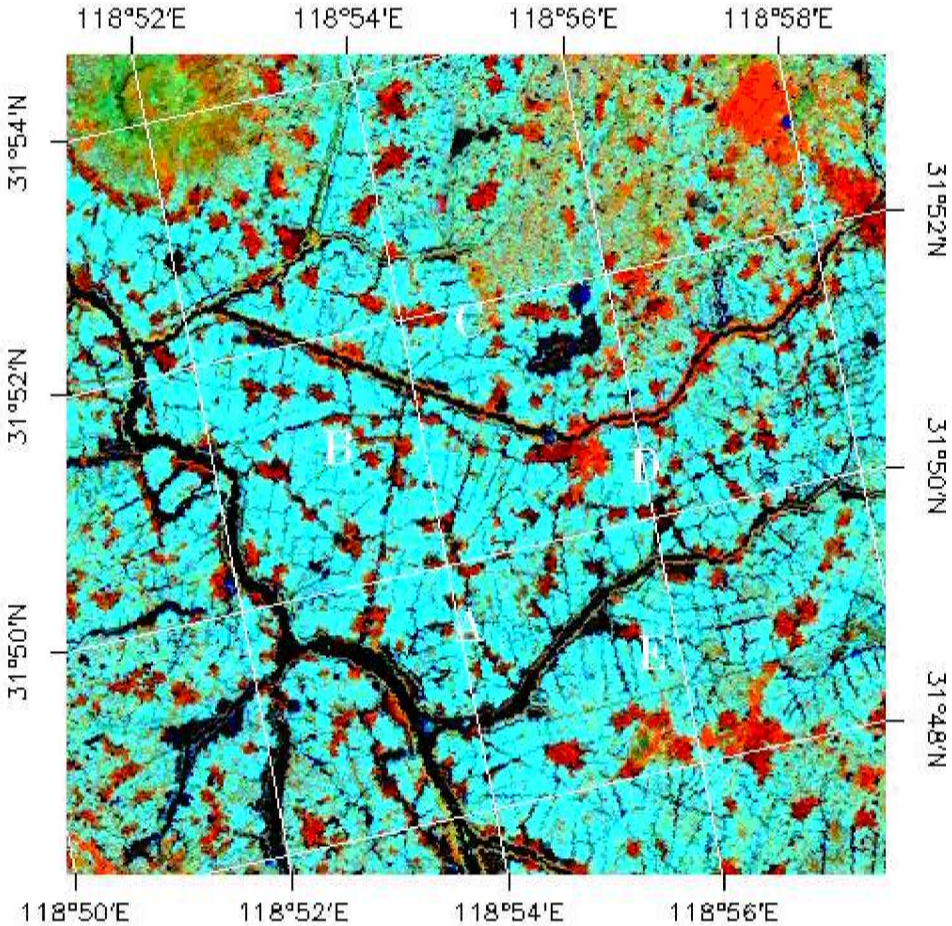

Figure 3. The locations of five intensive field sampling sites (A, B, C, D, E) in Jiangning County, Jiangsu Province, China. The background is a Landsat 5 TM image acquired on 22 April 1996, and is a false colour composite displayed with TM band 7 (red), NDVI (green) and NDWI (blue). For TM data, the NDVI is calculated as NDVI = (TM4 − TM3)/(TM4 + TM3), and the NDWI is calculated as NDWI = (TM4 − TM5)/(TM4 + TM5). The image is in Lambert Azimuthal Equal Area projection.

rice agriculture and usually takes place about one week to 10 days before rice transplanting. Rice seedlings (planted about 1 month earlier in small seed-bed nurseries) were transplanted in the flooded soil in mid-to-late June, and grew over the next 4 months (figure 4(*c* and *d*)). Soils were typically flooded for most of the rice season, with one or two short drainage/dry periods. Rice harvest occurred in late October and fields were immediately planted again for winter wheat or rapeseed. Field observations at 10-day intervals confirmed that crop management and growth on the selected fields were representative of paddy rice in the vicinity and thus of paddy rice within a 1-km^2 VGT pixel. These farm families kept records of the rice variety they planted, dates of seeding, dates of rice transplanting and harvesting, and fertilizer application in 1999 (table 2).

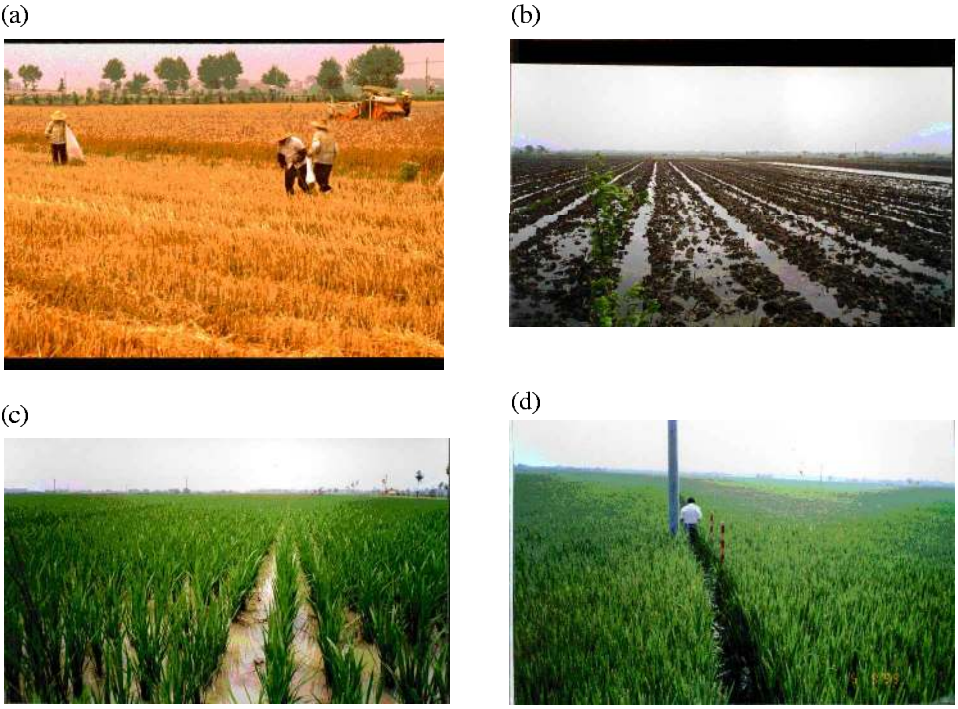

Figure 4. The crop rotation system from winter wheat to paddy rice in Jiangning County, Jiangsu Province, China. (*a*) Winter wheat harvesting, 2 June 1999; (*b*) paddy rice field preparation, 11 June 1999; (*c*) two weeks after rice transplanting, 3 July 1999; (*d*) Rice plant heading, 6 September 1999. Photos (*b*), (*c*) and (*d*) were taken at site C of figure 3, and photo (*a*) was taken nearby.

Table 2. Information collected in 1999 on seeding, transplanting, harvesting and fertilizing for the five sampling sites in Jiangning County, Jiangsu Province of China (also see figure 3).

	A	B	C	D	E
Longitude	118°54.519′	118°53.363′	118°54.76′	118°56.085′	118°55.861′
Latitude	31°49.623′	31°50.979′	31°51.613′	31°50.173′	31°48.68′
Farm size (mu*)	1.6	2.5	2.4	2.5	3.8
Seeding**	14 May	18 May	13 May	21 May	20 May
Transplanting	14 June	20 June	12 June	22 June	20 June
Harvesting	21 October	18 October	17 October	23 October	28 October
Fertilizing	20 June,	20 June,	11 June,	22 June,	20 June,
	30 July,	26 June,	19 June,	27 June,	26 June,
	9 August	31 July	1 August	29 July	28 July

*1 ha = 15 mu (Chinese area unit); **seeding occurs in small seedbeds, where rice seeds germinate and grow up to 10–20 cm tall before transplanting.

4. Results and discussion

4.1. *Temporal dynamics of NDWI and NDVI at the farm scale*

Winter wheat in the study area usually greens up in early March. NDVI and NDWI values were high in late April and early May at the five sampling sites

(figure 5). As winter wheat crops ripened, both NDVI and NDWI values gradually declined, probably because of decreases in photosynthetic pigments and water content. Before the harvest of winter wheat (late May to early June), both NDWI and NDVI had similar temporal dynamics among the five sampling sites and NDVI values were much larger than NDWI values (figure 5). Winter wheat was harvested in late May to early June. The post-harvest fields were primarily composed of crop residuals and exposed dry soils, and consequently both NDVI and NDWI dropped to very low values. Immediately after the harvest of winter wheat, farmers began land preparation for paddy rice cultivation, involving tilling and flooding of croplands. After the period of rice transplanting (mid-to-late June), rice plants accumulated both chlorophyll and water in their leaves/canopies. NDWI values increased gradually over time but NDVI values increased more rapidly at the early stage of the vegetative growth period (figure 5), probably because of rapid increases of green biomass and small changes in canopy moisture content in this period. There were similar temporal dynamics of NDWI and NDVI from early July to late October among the five sampling sites (figure 5). The MIR band of VGT is highly sensitive to leaf moisture and soil moisture, and the temporal dynamics of NDWI in both winter wheat and paddy rice highlighted the potential for using NDWI as a simple and effective tool for quantitatively estimating the water status of crop canopies.

It is important to note that on 11–20 June, NDVI values were smaller than NDWI values for all five sampling sites because of substantial increases of NDWI values but relatively little change in NDVI values from 1–10 June to 11–20 June (figure 5). At 1-km spatial resolution, land surface in the study area is mostly a mixture of water, vegetation and soils (figure 2(c, d)). The proportions of water, vegetation and soils within a 1-km^2 pixel vary over time and with different cropping systems. In comparison to winter wheat or rapeseed crop fields, paddy rice fields have a much larger proportion of surface water, especially during the period of flooding and rice transplanting. During initial flooding, there is a layer of surface water (approximately 2–10 cm deep) on the paddy rice fields. The observations that had smaller NDVI than NDWI values (or an NDVI/NDWI inversion) on 11–20 June corresponded well with the timing of land preparation and flooding for paddy rice fields. In the next composite (21–30 June), there was a slight decline in NDWI and a slight increase in NDVI (figure 5), which corresponded well with the timing of rice transplanting. Immediately after rice transplanting, the paddy rice fields were mostly a mixture of surface water and rice plants. The green rice canopy reduced the area of surface water observed from space. A reduction in exposed areas of surface water in the paddy rice fields after rice transplanting resulted in an increase of surface reflectance of the MIR band and, consequently, a slight decrease in NDWI values in the period of rice transplanting. The temporal changes in NDVI and NDWI from early to late June corresponded well with the crop shifts from winter wheat (non-flooded) to paddy rice (flooded) at all five sampling sites in Jiangning County.

4.2. *Temporal dynamics and spatial patterns of NDWI and NDVI at the landscape scale*

Based on the farm-scale analysis described above, our hypothesis is that NDVI/NDWI inversion (smaller NDVI than NDWI values) in mid- and late-June signalled flooding and rice transplanting in paddy fields. The key question at the landscape scale is to what extent VGT-derived NDWI and NDVI are capable of quantifying the spatial and temporal variations of flooding and rice transplanting of

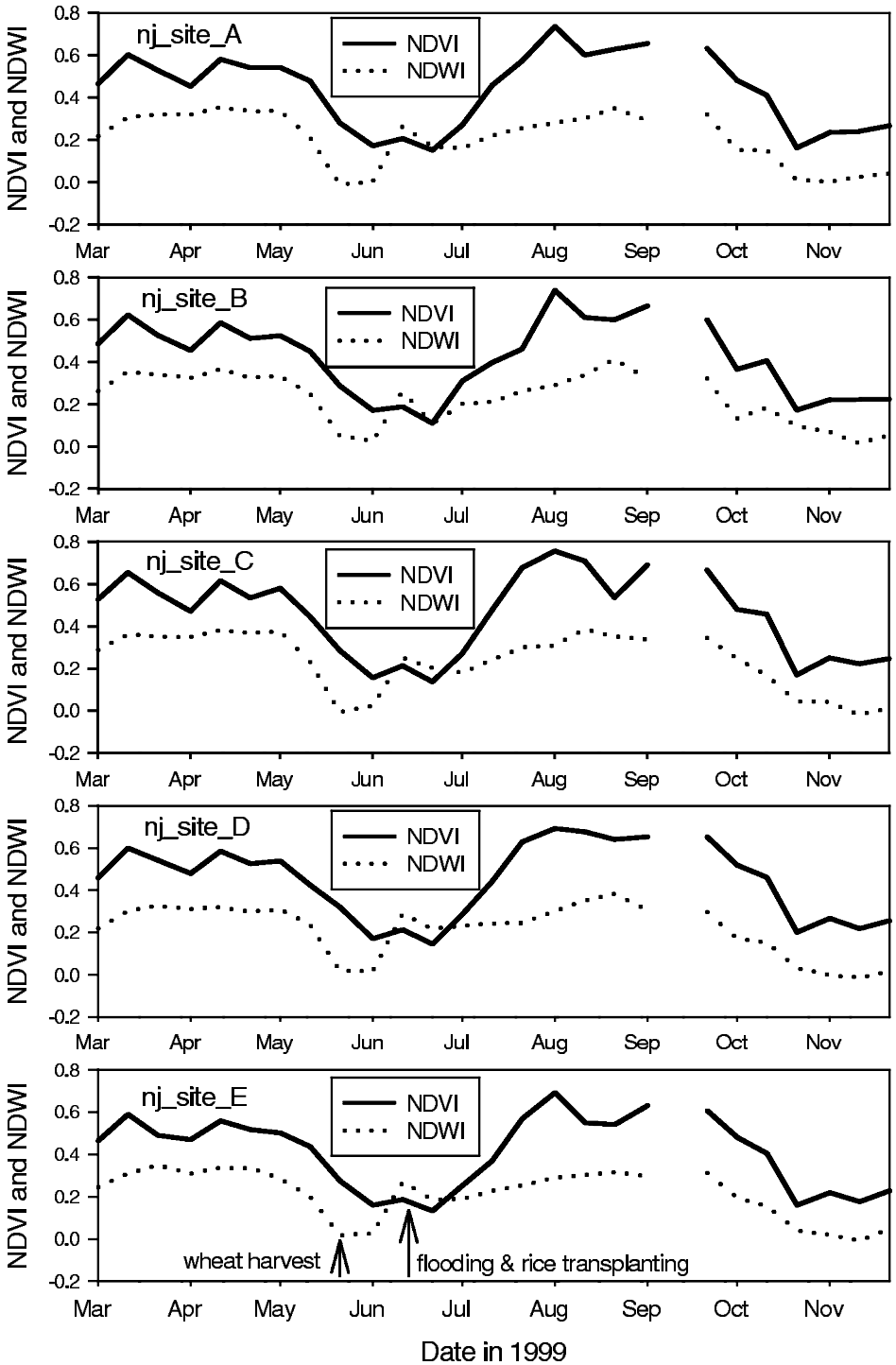

Figure 5. Temporal dynamics of the NDWI and the NDVI at the five sampling sites in Jiangning County, Jiangsu Province, China in 1999. Note that in 11–20 September 1999 there are no NDVI and NDWI data in the figure because there were no cloud-free VGT images for a large area of Jiangning County, including the five sampling sites.

paddy rice fields across a landscape mosaic of paddy and other crop (e.g. vegetables, cotton) and non-crop land uses (e.g. villages, roads, canals, forested hilltops). Individual farmers have different flooding and rice transplanting schedules for their paddy rice fields in the study area. However, these timing differences are constrained by environmental conditions and thus are most likely to be in the range of one to two weeks. Flooding and rice transplanting start as early as mid-June in this region of Jiangsu Province.

We calculated the difference between NDVI and NDWI of the entire study area (175 by 165 pixels or km^2) and counted numbers of VGT pixels that had smaller NDVI than NDWI values for each of the VGT S-10 composites (figure 6). The number of VGT pixels that had smaller NDVI than NDWI values increased substantially on 11–20 June, reached 7913 pixels on 21–30 June and quickly declined after that (figure 6). We selected four key periods (21–30 April, 11–20 June, 21–30 June and 1–10 August) for further comparison, based on local knowledge of cropping systems in the study area. A comparison of the histograms of NDVI and NDWI provides a simple but effective interpretation and summary of changes in the land surface (figure 7). Crop canopy of winter wheat and rapeseed crops had probably reached full closure by 21–30 April and, therefore, had high NDVI values. Similar to the NDVI dynamics observed in the five sampling sites, a large portion of the entire study area also had significant declines in mean NDVI values from 21–30 April to 21–30 June, as a result of the harvest of winter wheat and rapeseed crops. After the completion of rice transplanting, the mean NDVI values increased gradually. By 1–10 August, the crop canopy of paddy rice fields approached maximum leaf area index (LAI) (Xiao *et al.* 2002a) and the mean NDVI value of paddy rice fields was much larger than that during the winter wheat growing period (figure 7(a)).

In comparison with NDVI histograms, NDWI histograms have relatively narrower ranges of variation (figure 7(b)). In both the 21–30 April and 1–10 August periods, most of the VGT pixels had larger NDVI values than NDWI values. As

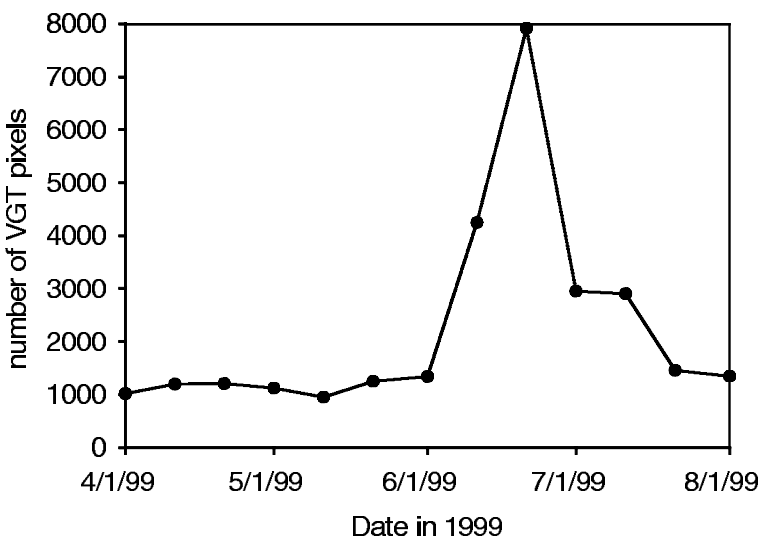

Figure 6. The number of VGT pixels that had smaller NDVI than NDWI values in the study area (175 by 165 pixels at 1-km spatial resolution) of Jiangsu Province, China, over the period 1–10 April to 1–10 August 1999.

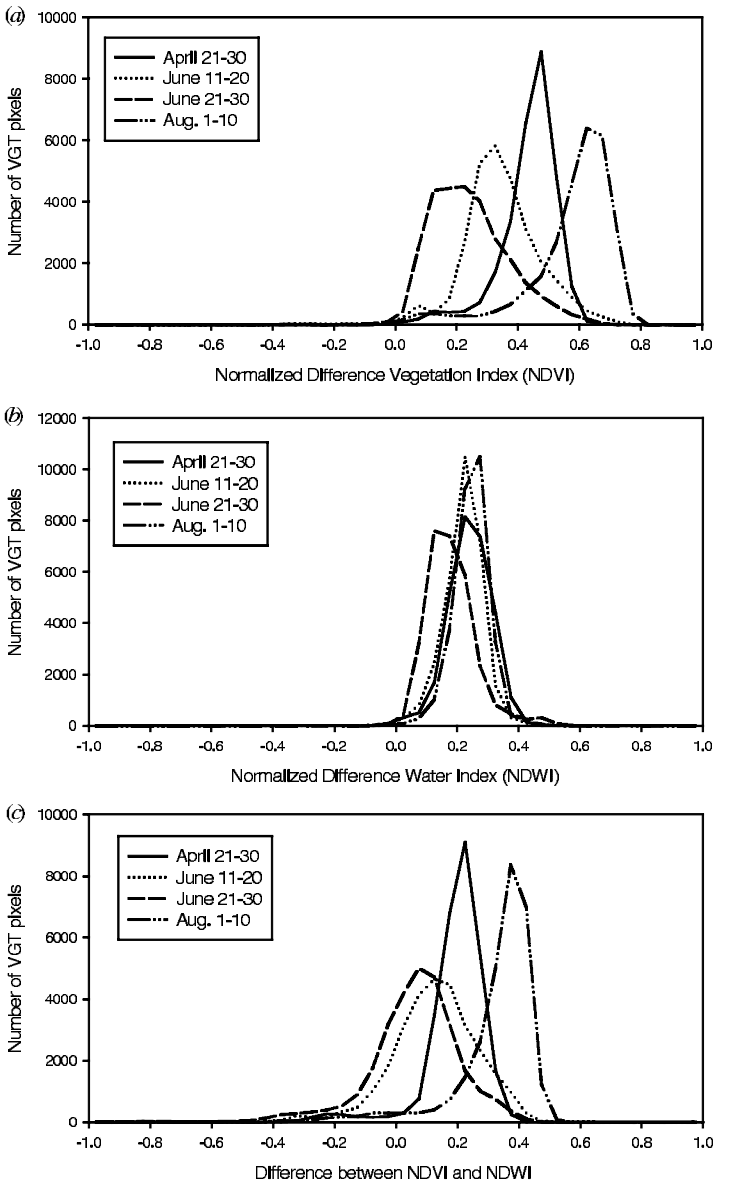

Figure 7. Histograms of (*a*) NDVI, (*b*) NDWI and (*c*) the differences between NDVI and NDWI in the study area (175 by 165 pixels at 1-km spatial resolution) of Jiangsu Province, China, for four VGT-S10 composites in 1999. The histograms were calculated using a bin size of 0.05.

shown in figures 6 and 7, there were substantial increases in VGT pixels that had smaller NDVI values than NDWI values in 11–20 June (4245 pixels) and 21–30 June (7913 pixels). This is consistent with the temporal NDVI and NDWI dynamics observed at the five sampling sites in Jiangning County (figure 5). The shift of histograms to the negative ranges (smaller NDVI than NDWI values) in 11–20 June and 21–30 June coincided well with the timing of flooding and rice transplanting in

the study area, and is attributed mostly to the sensitivity of the MIR band to leaf water content and soil moisture.

Maps of the differences between NDVI and NDWI values for the study area were generated and compared (figure 8). The map of the difference between NDVI and NDWI values on 21–30 April (figure 8(*a*)) highlights the spatial distribution of those pixels that are dominated by surface water bodies (e.g. the Yangtze River, lakes). As shown in figures 2(*d*) and 8(*b*, *c*), most of those pixels that had negative values (smaller NDVI than NDWI values) on 11–20 June and 21–30 June had large proportions of croplands as estimated by Landsat TM image classification (Xiao *et al.* 2002b), and corresponded well with the timings of land preparation, flooding and rice transplanting at paddy rice fields in the study area. By 1–10 August, paddy rice fields had already approached full closure of the crop canopy (Xiao *et al.* 2002a) and had high NDVI and NDWI values, and positive difference values between NDVI and NDWI (figure 8(*e*)). Therefore, by August, the areas with negative difference values between NDVI and NDWI again highlighted those pixels with large proportions of surface water bodies.

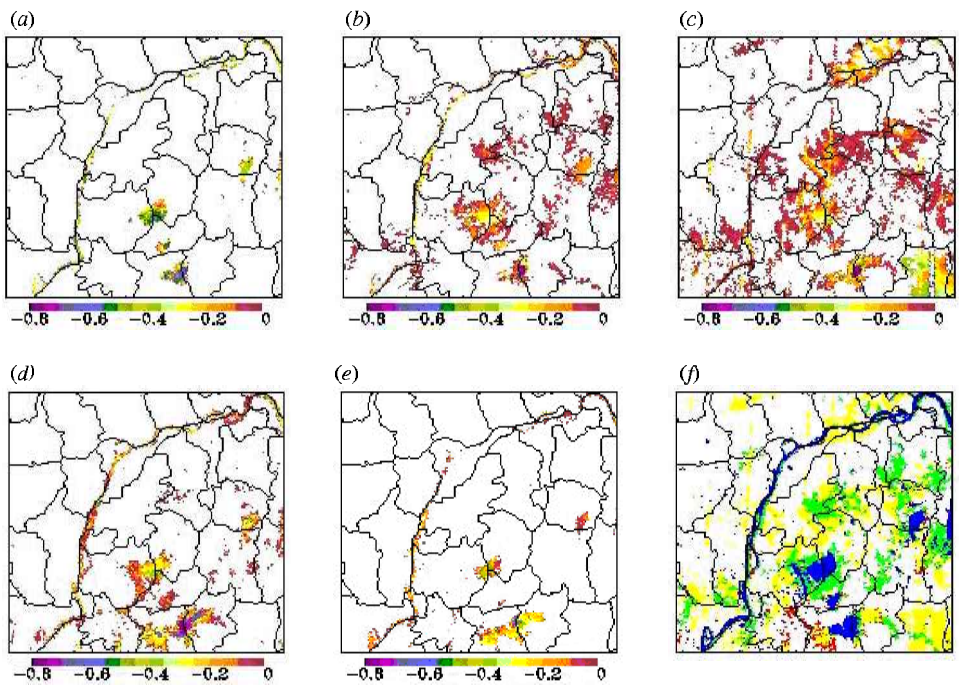

Figure 8. Maps for the differences between NDVI and NDWI values: (*a*) 21–30 April 1999; (*b*) 11–20 June 1999; (*c*) 21–30 June 1999; (*d*) 1–10 July 1999; (*e*) 1–10 August 1999. Note that all those pixels that have larger NDVI values than NDWI values are coloured white. In this way, the graph emphasizes those pixels that have smaller NDVI values than NDWI values. (*f*) Thematic map for the timings of flooding and rice transplanting in the study area (175 by 165 pixels at 1-km spatial resolution) of Jiangsu Province, China. Colour code in the land use thematic map is as follows: blue, surface water bodies; green, flooding and rice transplanting in 11–20 June 1999; yellow, flooding and rice transplanting in 21–30 June 1999; red, flooding and rice transplanting in 1–10 July 1999; white, other land. The geographical area in figure 8 is the same as in figure 2.

Based on the above spatial–temporal analysis of NDWI and NDVI, a land use thematic map for the timing of flooding and rice transplanting in the study area was generated (figure 8(*f*)). According to the aggregated classification results from Landsat TM imagery (figure 2(*c*); Xiao *et al.* 2002b), the study area has 2072 VGT pixels that have more than 40% surface water bodies within a 1-km^2 pixel. In generating such a land use thematic map, we first masked out those water body pixels (>40% water bodies within a 1-km^2 pixel), as estimated by Landsat TM imagery analysis (figure 2(*c*); Xiao *et al.* 2002b), and then assigned the remaining pixels that had smaller NDVI values than NDWI values in 11–20 and 21–30 June and 1–10 July to be flooded paddy rice fields. It is estimated that flooding and rice transplanting took place in 2957 pixels (km^2) on 11–20 June, 4852 pixels (km^2) on 21–30 June and 428 pixels (km^2) on 1–10 July, resulting in a total of 8237 pixels (km^2) in the study area (figure 8(*f*)). About 85% of these 8237 VGT pixels have more than 30% cropland within a 1-km^2 pixel (figure 2(*d*)). According to the aggregated classification results of the Landsat TM imagery analysis (figure 2(*d*); Xiao *et al.* 2002b), the study area had 7642 pixels (km^2) that had $\geqslant$60% cropland within a 1-km^2 pixel, and 11 840 pixels (km^2) that had $\geqslant$50% cropland within a 1-km^2 pixel. In general, the spatial pattern of flooding and rice transplanting (figure 8) corresponded well with the spatial distribution of croplands as estimated by Landsat TM image analysis (figure 2(*d*)).

5. Summary

This analysis of multi-temporal VGT data at farm and landscape scales has shown that the VGT-derived NDWI values were sensitive enough to capture the significant increases of surface water in croplands, following a physical system shift from non-flooded agriculture (winter wheat, rapeseed) to flooded agriculture (paddy rice) in the study area. We did not conduct extensive field surveys in 1999 to quantitatively verify the VGT analysis for the timings of flooding and rice transplanting, but the results are qualitatively consistent with field observations at the five sampling sites and with local farming practices. In short, the results of this study indicate that the NDVI and NDWI temporal anomaly in the time series of VGT images may provide a simple and effective tool for operationally identifying the flooding and rice transplanting at paddy rice fields across the landscape to regional scales.

Acknowledgments

This project was supported by the US multi-agency Terrestrial Ecology and Global Change (TECO) program, and the NASA Earth Observing System (EOS) Interdisciplinary Sciences (IDS) program. We thank the two anonymous reviewers for their insightful comments and suggestions on the earlier version of the manuscript.

References

Bachelet, D., 1995, Rice paddy inventory in a few provinces of China using AVHRR data. *Geocarto International*, **10**, 23–38.

Denier Van Der Gon, H., 2000, Changes in CH4 emission from rice fields from 1960s to 1990s. 1. Impacts of modern rice technology. *Global Biogeochemical Cycles*, **1**, 61–72.

Fang, H., 1998, Rice crop area estimation of an administrative division in China using remote sensing data. *International Journal of Remote Sensing*, **17**, 3411–3419.

Fang, H., Wu, B., Liu, H., and Xuan, H., 1998, Using NOAA AVHRR and Landsat TM to estimate rice area year-by-year. *International Journal of Remote Sensing*, **3**, 521–525.

Gao, B., 1996, NDWI—A normalized difference water index for remote sensing of vegetation liquid water from space. *Remote Sensing of Environment*, **58**, 257–266.

Gao, L., Jin, Z., Wang, Y., Chen, H., and Li, B. (eds), 1992, *Rice Cultivation Simulation-Optimization-Decision Making System (RCSODS)* (Beijing: Press of Agricultural Science and Technology) (in Chinese).

Le Toan, T., Ribbes, F., Wang, L., Floury, N., Ding, K., Kong, J., Fujita, M., and Kurosu, T., 1997, Rice crop mapping and monitoring using ERS-1 data based on experiment and modeling results. *IEEE Transactions on Geoscience and Remote Sensing*, **1**, 41–56.

Lu, D. (ed.), 1997, *Applications of Remote Sensing Technology in Agricultural Engineering*. (Beijing: Qinghua University Press) (in Chinese).

Martin, R. D. Jr, and Heilman, J. L., 1986, Spectral reflectance patterns of flooded rice. *Photogrammetric Engineering and Remote Sensing*, **52**, 1885–1897.

Miller, B. C., Foin, T. C., and Hill, J. E., 1993, CARICE: a rice model for scheduling and evaluating management actions. *Agronomy Journal*, **4**, 938–947.

Neue, H., and Boonjawat, J., 1998, Methane emissions from rice fields. In *Asian Change in the Context of Global Climate Change*, edited by J.N. Galloway and J.M. Melillo (Cambridge: Cambridge University Press), pp. 187–209.

Okamoto, K., and Fukuhara, M., 1996, Estimation of paddy rice field area using the area ratio of categories in each pixel of Landsat TM. *International Journal of Remote Sensing*, **9**, 1735–1749.

Okamoto, K., and Kawashima, H., 1999, Estimating of rice-planted area in the tropical zone using a combination of optical and microwave satellite sensor data. *International Journal of Remote Sensing*, **5**, 1045–1048.

Rahman, H., and Dedieu, G., 1994, SMAC: a simplified method for atmospheric correction of satellite measurements in the solar spectrum. *International Journal of Remote Sensing*, **15**, 123–143.

Tennakoon, S. B., Murty, V. V. N., and Etumnoh, A., 1992, Estimation of cropped area and grain yield of rice using remote sensing data. *International Journal of Remote Sensing*, **13**, 427–439.

Tucker, C. J., 1980, Remote sensing of leaf water content in the near-infrared. *Remote Sensing of Environment*, **10**, 23–32.

Wang, Y., Gao, L., Jin, Z., and Chen, H., 1996, A software package for optimizing rice production management based on growth simulation and feedback control. *Agricultural Systems*, **4**, 335–354.

Xiao, X., He, L., Salas, W., Li, C., Moore, B., Zhao, R., Frolking, S., and Boles, S., 2002a, Quantitative relationships between field-measured leaf area index and vegetation index derived from VEGETATION images for paddy rice fields. *International Journal of Remote Sensing* (in press).

Xiao, X., Boles, S., Frolking, S., Salas, W., Moore III, B., Li, C., He, L., and Zhao, R., 2002b, Landscape-scale characteristics of cropland in China using VEGETATION and Landsat TM images. *International Journal of Remote Sensing* (in press).

Zhao, R., Wang, Y., and Dai, J. (eds), 1996, *Dynamic Monitoring and Production Estimation of Paddy Rice Agriculture in China* (Beijing: Press of Science and Technology) (in Chinese).